

Second Virial Coefficient For Real Gases At High Temperature*

H. Boschi-Filho^{†‡} and C.C.Buthers[‡]

[†] *Center for Theoretical Physics, Laboratory for Nuclear Science
Massachusetts Institute of Technology
Cambridge, Massachusetts 02139-4307, USA*

and

[‡] *Instituto de Física, Universidade Federal do Rio de Janeiro
Cidade Universitária, Ilha do Fundão, Caixa Postal 68528
21945-970 Rio de Janeiro, BRAZIL*

January 24, 1997

Abstract

We study the second virial coefficient, $B(T)$, for simple real gases at high temperature. Theoretical arguments imply that there exists a certain temperature, T_i , for each gas, for which this coefficient is a maximum. However, the experimental data clearly exhibits this maximum only for the Helium gas. We argue that this is so because few experimental data are known in the region where these maxima should appear for other gases. We make different assumptions to estimate T_i . First, we adopt an empirical formulae for $B(T)$. Secondly, we assume that the intermolecular potential is the Lennard-Jones one and later we interpolate the known experimental data of $B(T)$ for Ar , He , Kr , H_2 , N_2 , O_2 , Ne and Xe with simple polynomials of arbitrary powers, combined or not with exponentials. With this assumptions we estimate the values of T_i for these gases and compare them.

PACS: 34.20.-b; 05.70.Ce; 65.50.+m; 33.15.-e.

*This work is supported in part by funds provided by the U.S. Department of Energy (D.O.E.) under cooperative research agreement #DF-FC02-94ER40818 and Conselho Nacional de Desenvolvimento Científico e Tecnológico (CNPq) - Brazilian agency.

[†]E-mail address: boschi@ctp.mit.edu

1 Introduction

Long time ago, Kamerlingh Onnes and collaborators performed a systematical study of physical properties of gases at low temperature, measuring their deviations from the ideal gas law, or in other words, determining their virial coefficients [1]-[3]. Since then, much research has been done in this direction collecting more and more data for many different substances, mainly at low temperature [4]. In particular, in 1925, Holborn and Otto studied some simple gases (Ar, He, H₂, N₂, and Ne) and they were able to determine an empirical formula for the second virial coefficient, $B(T)$, which constituted at that time and persists until today as a land-mark work in physics [5].

On the other hand and at the same time, Lennard-Jones showed in another remarkable work that for intermolecular potentials written as binomials of arbitrary powers of the intermolecular distance, the corresponding second virial coefficient $B(T)$ can be calculated exactly as an infinite power series [6]. This kind of potential describes very well the behavior of simple molecules as the one studied by Kamerlingh Onnes, Holborn and Otto and others. Also, other types of intermolecular potentials have been discussed but without exact integrability [7]. Despite of the long time that these empirical and theoretical expressions for $B(T)$ are known, they are usually not equal. This can be understood paying attention to the fact that the experimental data available for most substances are restricted to a certain range of temperatures, usually below $600K$. The choice for low temperature physics seems rather natural if one, for example, is looking for critical phenomena in condensed matter which can be almost entirely found in this region. However, the high temperature behavior of real gases can also be of interest, for example, in the study of hot plasma and in many situations in astrophysics as nucleosynthesis, super-novae, etc.

Here in this paper, we are going to examine the second virial coefficient of some real simple gases (Ar, He, Kr, H₂, N₂, O₂, Ne and Xe) at high temperature. This is not an easy task since few data for these and other gases are available for temperatures above the range $600 \sim 1000K$. The main point of this work is that we can show from measures

of $B(T)$ that most of these real simple gases admits a maximum value corresponding to a certain temperature for each gas, which may be called an inversion temperature (T_i). The existence of this maximum may be not a surprise once it is already present, for the Helium, in Holborn and Otto work [5]. However, for all other real gases they are not yet known. Anyway, some previous discussions on this maximum [8] and on this inversion temperature [9] can be found in the literature.

This paper is organized as follows: in section 2, we discuss the inversion temperature T_i associated with the Joule or free expansion and recall the well known inversion temperature related to the Joule-Thomson throttling process, T_{iJT} . We show that there is a kind of duality between the equations governing these two temperatures. The temperatures T_{iJT} are known experimentally and can also be obtained by various theoretical methods, one of them assumes the knowledge of an equation of state. We show, however, that the known equations of state do not lead to any finite T_i . In section 3, we employ different methods to estimate the inversion temperature T_i . The first and simplest one is to use the empirical expression for $B(T)$ given by Holborn and Otto from which we can find easily its maximum. The second and third methods are based on the assumption that the intermolecular potential between the molecules of the real gas is the Lennard-Jones 6-12 potential [6]. So, the second method consists in finding the inversion temperature T_i evaluating $dB/dT = 0$ numerically. The third method is a variation of the second since the assumption of the Lennard-Jones potential permit us to relate the temperatures T_i and T_{iJT} , determining the former, once the latter are well known. The fourth and last method for determining T_i , that we discuss in this paper, is a numerical analysis of the experimental data for $B(T)$ for the above mentioned gases. We interpolate these data with simple polynomial functions with arbitrary powers with and without exponentials terms. In section 4, we compare the results obtained from these functions with the ones from other methods and present our conclusions.

2 The Inversion Temperatures T_i and T_{iJT}

The inversion temperature T_i , for which $B(T)$ is a maximum, has a simple physical interpretation. A real gas, initially at this temperature, subjected to a free expansion remains at this temperature for any change in its volume, which is the ideal gas behavior, for any initial temperature. If the real gas initial temperature is greater than T_i then it will get hotter in a free expansion and the reverse occurs if $T < T_i$, which is our "daily" experience. One can understand this simply by noting that the Joule coefficient, i.e., the variation of temperature against volume in a free expansion (with internal energy U being constant) can be expressed as [10]

$$J \equiv \left(\frac{\partial T}{\partial V}\right)_U = \frac{1}{c_V} \left[P - T \left(\frac{\partial P}{\partial T}\right)_V \right]. \quad (2.1)$$

Writing the virial expansion as

$$PV = RT \left(1 + \frac{B}{V} + \frac{C}{V^2} + \frac{D}{V^3} + \frac{E}{V^4} + \dots \right) \quad (2.2)$$

it is easy to show that, in the thermodynamical limit ($V \rightarrow \infty$)

$$J = -\frac{RT^2}{c_V V^2} \left(\frac{dB}{dT} \right), \quad (2.3)$$

where $B \equiv B(T)$. Looking at the above expression one can see that the maximum of $B(T)$, which may occur for certain values of $T = T_i$, vanishes the Joule coefficient J :

$$J = 0 \quad \Leftrightarrow \quad \frac{dB}{dT} = 0. \quad (2.4)$$

Assuming that T_i is unique, above this temperature J will be positive and so the temperature increases under a free expansion. Below T_i the temperature decreases.

In fact, this behavior is also expected in the bases of the Yang and Lee Theorem [11] (see also [8]) if one assumes that the intermolecular potential of the gas has a shape as the one given by fig.1. This is a typical shape which includes the well known Lennard-Jones, Stockmayer and other potentials [7]. This kind of potential implies a maximum for

$B(T)$ since they are not infinite for finite distances between molecules, contrary to what happens for the hard-sphere case, for example.

At this point, it is interesting to discuss a well known inversion temperature, T_{iJT} , that one associated with the Joule-Thomson throttling process with constant enthalpy and its relation to the previous discussed inversion temperature T_i . The relevant coefficient in this case can be written as [10]

$$\mu = \frac{1}{c_P} [T \left(\frac{\partial V}{\partial T} \right)_P - V]. \quad (2.5)$$

As the derivative of the volume in respect to the temperature must be calculated under constant pressure, the virial expansion (2.2) is not the most appropriate in this case and it is usual to rewrite it as

$$PV = RT(1 + B_P P + C_P P^2 + D_P P^3 + E_P P^4 + \dots), \quad (2.6)$$

so we get immediately, in the low pressure limit ($P \rightarrow 0$)

$$\mu = \frac{RT^2}{c_P} \left(\frac{dB_P}{dT} \right). \quad (2.7)$$

The inversion temperature, in this process, T_{iJT} , is determined by the vanishing μ :

$$\mu = 0 \quad \Leftrightarrow \quad \left. \frac{dB_P}{dT} \right|_{T=T_{iJT}} = 0. \quad (2.8)$$

These temperatures, apart from being well known for most real gases, are of great practical importance, for example, to improve the efficiency of thermal engines as refrigerators [12]. Another striking property of this temperature is its resemblance with T_i . This is not a coincidence since the second virial coefficients at constant volume and pressure, B and B_P , respectively, are simply related by

$$B = B_P RT. \quad (2.9)$$

So, we can trace a parallel between these two inversion temperatures first substituting the above expression into eq.(2.7) so we get

$$\mu = 0 \quad \Leftrightarrow \quad \frac{dB}{dT} = \frac{B}{T}; \quad T = T_{iJT}, \quad (2.10)$$

which is the usual expression for the throttling process [7] and then into eq. (2.3)

$$J = 0 \quad \Leftrightarrow \quad \frac{dB_P}{dT} = -\frac{B_P}{T}; \quad T = T_i, \quad (2.11)$$

for the Joule expansion. Comparing eqs. (2.4) and (2.8), (2.10) and (2.11) one can see clearly a kind of duality between the equations governing these two processes: The role played by the inversion temperature T_{iJT} in the constant enthalpy process is analogous to the T_i in the constant energy case. Despite of this appealing resemblance the inversion temperature T_i for the Joule process has been rarely discussed [9], and these discussions are far from being satisfactory or complete.

The temperatures T_{iJT} are known experimentally and can also be estimated using simple equations of state [10]. One can wonder if the inversion temperature T_i can be found from equations of state as happens for T_{iJT} . This should be nice, but for various equations of state the corresponding second virial coefficient does not allow any finite T_i , as can be seen by inspection of Table 1. Note that $B(T)$ for the Beattie-Bridgeman equation of state admits in principle a maximum, but actually as the values of the constants a and c are positive for real gases one finds that no real T_i are admissible from this equation too.

3 Estimates On The Inversion Temperature T_i

There are various possible ways of computing T_i . We will discuss some of them and compare their results. If one knows the correct expression for $B(T)$ then the problem would be trivial, since the equation $dB/dT = 0$ could be solved immediately. But what we have until now are, on one side expressions for $B(T)$ based on theoretical assumptions and on the other side empirical expressions which differ in general from each other and are constructed on the data for which the temperatures are low, usually under $600K$. As we are going to show, these maxima appear in a region beyond this temperature, except for the Helium, for which $T_i \simeq 200K$ [5].

Among the known expressions for $B(T)$, the most simple is, perhaps, the Holborn and Otto [5] one

$$B(T) = a + bT + \frac{c}{T} + \frac{e}{T^3}, \quad (3.1)$$

from which one can easily find that the inversion temperature, in this case is given by

$$T_i = \sqrt{\frac{c - \sqrt{c^2 + 12eb}}{2b}}. \quad (3.2)$$

The values of the coefficients appearing in eq. (3.1) and the corresponding T_i 's for some simple gases are found in Table 2.

From statistical mechanics, it is well known that an intermolecular potential, $u(\vec{r})$, and the corresponding the second virial coefficient are related by:

$$B(T) = \frac{1}{2} \int_V d\vec{r} [1 - \exp(-u(\vec{r})/kT)], \quad (3.3)$$

where k is the Boltzmann constant. So, the inversion temperature T_i could also, in principle, be obtained analytically through this expression. However, this is a formidable task for almost of known intermolecular potentials except from the trivial ones like the hard-sphere, which does not imply any finite T_i . An important exception is the Lennard-Jones potential [6]:

$$u_{LJ}(r) = \epsilon_0 [(\frac{r_0}{r})^{12} - 2(\frac{r_0}{r})^6], \quad (3.4)$$

for which $B(T)$ can be computed exactly as an infinite power series. The constants ϵ_0 and r_0 are tabulated for many real gases. Substituting (3.4) into (3.3) one can show that [7]

$$B(T) = b_0 \sum_{j=0}^{\infty} b^{(j)} T^{*- \frac{(2j+1)}{4}}, \quad (3.5)$$

where $T^* = \frac{kT}{\epsilon_0}$ is the reduced temperature, $b_0 = \frac{\sqrt{2}}{3} \pi \tilde{n} r_0^3$, \tilde{n} being the number of molecules per mol and

$$b^{(j)} = -\frac{2^{j+\frac{1}{2}}}{4j!} \Gamma(\frac{2j-1}{4}). \quad (3.6)$$

The importance of this potential is related to the fact that it describes the Van der Waals force of attraction between molecules, which is proportional to r^{-7} (in the non-relativistic limit) and includes a finite repulsion at small finite distances, being integrable and fitting (low temperature) data quite well for a great number of real gases. For this potential, we can evaluate the inversion temperature T_i , since

$$\frac{dB(T)}{dT} = -\frac{\epsilon_0 b_0}{kT^*} \sum_{j=0}^{\infty} \frac{(2j+1)}{4} b^{(j)} T^{*- \frac{(2j+1)}{4}} \quad (3.7)$$

and imposing that

$$\frac{dB(T)}{dT} = 0, \quad (3.8)$$

which solution can be evaluated numerically. As the expected inversion temperature is of order $10^2 \sim 10^3 K$, we see that the series in eq.(3.7) is rapidly convergent. Taking $j = 5$ we find

$$T_i^* = \frac{kT_i}{\epsilon_0} \cong 25.152 \quad (3.9)$$

with precision of 0.001. If we extend this calculation until $j = 15$, for example, it will change less than 0.001 (see Table 3). Using the data for ϵ_0 from [7] in the above equation, we can estimate the inversion temperature for mono-atomic and diatomic (and perhaps for simple poly-atomic gases) which results can be seen in Table 4.

A related analysis can also be made for the inversion temperature T_{iJT} of the throttling process. Starting from the expression for $B(T)$, eq. (3.5), corresponding to the Lennard-Jones potential and imposing the conditions (2.10) we find (see Table 3)

$$T_{iJT}^* = \frac{k}{\epsilon_0} T_{iJT} \cong 6.431 \quad (3.10)$$

As these temperatures are well known, comparing eqs.(3.9) and (3.10) we can also find T_i from them:

$$T_i \simeq 3.911 T_{iJT}, \quad (3.11)$$

when we assume that the intermolecular potential is the Lennard-Jones one. The temperatures calculated using this relation are shown in Table 5. These numerical results could

also be inferred from tabulated values of $B(T)$ and its derivatives for the Lennard-Jones potential [7] (see also [9]).

As our last method for computing T_i , we will consider polynomial expressions for $B(T)$, combined or not with exponential terms, which parameters will be fixed by best fitting of experimental data from [4]. The first and simplest case is

$$B_1(T) = \frac{a}{T^b} + \frac{c}{T^d} \quad (3.12)$$

and we will use Powell's method from *Numerical Recipes* [14] to minimize χ^2 , defined by

$$\chi^2 = \sum_{n=1}^N [B_L(T_n) - B_{exp}(T_n)]^2 \quad (3.13)$$

where $B_L(T_n)$, with $L = 1$, is the expression (3.12) calculated with N experimental temperature values T_n , ($n = 1, \dots, N$) and $B_{exp}(T_n)$ are the corresponding experimental values for the second virial coefficient. In Table 6, we give the coefficients of (3.12) which minimize χ^2 for each gas and present the inversion temperature T_i calculated from them. In fact, except for the Helium, these values of T_i correspond to extrapolations on the interpolated expressions of $B_1(T)$.

In order to improve these results we also consider other functions for $B(T)$, which are

$$B_2(T) = \frac{a}{T^b} + \frac{c}{T^d} + \frac{e}{T^f} \quad (3.14)$$

$$B_3(T) = \frac{a}{T^b} + \frac{c}{T^d} + f \exp(-gT) \quad (3.15)$$

$$B_4(T) = \frac{a}{T^b} + \frac{c}{T^d} + \frac{e}{T^f} + g \exp(-hT). \quad (3.16)$$

and repeat the above procedure, as was done for $B_1(T)$. The corresponding results for $B_2(T)$, $B_3(T)$ and $B_4(T)$ are shown in Tables 7, 8 and 9, respectively. The data we have used for $B(T)$ for these gases are the ones which were compiled by Dymond and Smith [4]. In particular, for the Argon we used $N = 36$ experimental data from [5], [15], [16] and [17]. For the Helium we used $N = 31$ experimental data from [5],[18], [19] and [20]. For the Krypton we used $N = 28$ experimental data from [21], [22] and [23]. For the Hydrogen

we used $N = 30$ experimental data from [1], [5], [15] and [24]. For the Nitrogen we used $N = 38$ experimental data from [3], [5], [19] and [25]. For the Neon we used $N = 19$ experimental data from [5] and [26]. For the Oxygen we used $N = 20$ experimental data from [2], [5], [27] and [28]. Finally, for the Xenon we used $N = 30$ experimental data from [29], [30] and [31].

To get more confidence on these results, we have also shown them graphically in figures 2 to 9. In these figures we have plotted the best fitting for eqs. (3.12) and (3.14) - (3.16), for each gas separately. Note that for the most of gases only one curve can be seen since the fittings are very close to each other. In particular, in fig. 3 (Helium) three different curves can be seen, corresponding to the equations (3.12) and (3.14) - (3.16). In this case the fitting represented by eqs. (3.15) and (3.16) are very close to each other.

4 Discussion and Conclusions

We have estimated the inversion temperature T_i related to the Joule or free expansion by different methods. As can be seen from tables 2 and 4 to 9, each gas has a different inversion temperature T_i , which depend also on the method employed. In some cases as for the Hydrogen the values found can differ by a factor of 2 and for the Nitrogen by 4. Another gases as the Helium and Argon the discrepancy was about a factor of 5/3 and 3/2, respectively. Taking this into account and using a χ^2 -weighted average, we estimate a value for T_i corresponding to each gas, basically from the numerical fitting expressed in Tables 6 – 9, which results can be seen in Table 10. The choice for taking only the temperatures from Tables 6 – 9 is based on the fact that the values from these tables are the ones in which minimum modeling assumptions were made, since we left the powers of the polynomials (3.12) and (3.14) - (3.16) to be fixed by best fitting to experimental data, contrary to what happens in the other methods that we discussed before. Looking at Table 10 one can also see that for the Oxygen and Krypton we could not find values for T_i , despite that from Tables 4 and 5 we can see, by other methods some values for them.

To give an idea of the global behavior of the expressions for $B(T)$ and to visualize some of the maxima corresponding to the inversion temperature T_i discussed above, we have plotted in a single graph (see fig. 10) the shape of eq. (3.16) which we found for all the gases discussed in this paper until temperatures of the order of $4 \times 10^3 K$. As one can see from this graph some gases as the Helium, of course, and the Hydrogen exhibits clearly these maxima. For some others as the Neon, Argon and Nitrogen these maxima can be seen in a careful analysis, while for the Krypton, Xenon and Oxygen they can not be seen in this range of temperatures.

To conclude, we can say that the inversion temperature T_i associated with the free expansion of a real gas can be determined for some simple gases and in general they were not known because there are few experimental data for the range of temperatures in which they should appear. Despite that the physical interpretation of the inversion temperature T_i is related to a free expansion which is a non-equilibrium process and so difficult to analyze directly, the values for $B(T)$ can be taken from usual PVT measures. An important consequence of determining precisely this inversion temperature is that it will permit a greater confidence between the experimental and theoretical expressions for $B(T)$ and consequently on the force between molecules.

Acknowledgments: We would like to acknowledge F.M.L. de Almeida, A.S. de Castro and Y.A. Coutinho for the help with different computational parts of this work and specially A. Ramalho who wrote a Fortran program which enable us to use the Powell routine of *Numerical Recipes*. H.B.-F. acknowlegdes R. Jackiw for his hospitality at MIT and for reading the manuscript and K. Huang for an interesting discussion on these results. The authors were partially supported by CNPq – Brazilian agency (C.C.B. under the CNPq/PIBIC program).

References

- [1] H.Kamerlingh Onnes and C.Braak, Communs Phys. Lab. Univ. Leiden, **100b**,(1907).
- [2] H. A. Kuypers and H. Kamerlingh Onnes, Archs neerl. Sci., **6**,277,(1923).
- [3] H. Kamerlingh Onnes and A. T. van Urk, Communs Phys. Lab. Univ. Leiden, **169d**,
e,(1924).
- [4] A compilation of the virial coefficients for many different substances can be found in:
J. H. Dymond and E. B. Smith,*The Virial coefficients of Pure Gases and Mixtures*.
Oxford, Clarendon, (1980).
- [5] L. Holborn and J. Otto, Z. Physik **33**,1,(1925).
- [6] J. E. Lennard-Jones, Proc. Roy. Soc. , London, **A106**, 463, (1924).
- [7] For a review see: J. O. Hirschfelder, C. F. Curtiss and R. B. Bird, *Molecular theory
of gases and Liquids*. New York, Wiley, (1954).
- [8] S. K. Ma, *Statistical Mechanics*. Singapore, World Scientific, (1985).
- [9] B. Roulet and J-O. Goussard, Am. J. Phys. **61**, 845, (1993).
- [10] See *e. g.* G. W.Castellan, *Physical Chemistry*, 2nd. ed. Reading, Addison-Wesley,
(1971).
- [11] C. N. Yang and T. D. Lee, Phys. Rev., **87**, 404, (1952).
- [12] See *e. g.* F. C. Andrews, *Thermodynamics: Principles and Applications*, New York,
Wiley, (1971).
- [13] A. Kestin, *Course in Statistical Thermodynamics*. New York, Academic, (1971).
- [14] W.H. Press, S.A. Teukolsky, W.T. Vetterling and B.P. Flannery, *Numerical Recipes
in Fortran*, 2nd ed. Cambridge Univ. Press, 1992.

- [15] C. C. Tanner and I. Masson, Proc. R. Soc., **A126**, 268, (1930).
- [16] E. Whalley, Y. Lupien and W. G. Schneider, Can. J. Chem., **31**,722,(1953).
- [17] B. E. F. Fender and G. D. Halsey,Jr., J. Chem. Phys.,**36**,1881,(1962).
- [18] D. White, T. Rubin, P. Camky and H. L. Johnston, J. Phys. Chem., Ithaca **64**,1607,(1960).
- [19] R. J. Witonsky and J. G. Miller, J. Am. Chem. Soc., **85**,282,(1963).
- [20] N.K. Kalfoglou and J.G. Miller, J. Phys. Chem., Ithaca **71**,1256,(1967).
- [21] J. A. Beattie, J. S. Brierley and R. J. Barriault, J. Chem. Phys.,**20**,1615,(1952).
- [22] E. Whalley and W. G. Schneider, Trans. Am. Soc. Mech. Engng., **76**,1001,(1954).
- [23] H. P.Rentschler and B.Schramm, Ber.(dtsh) Bunsenges. Phys. Chem.,**81**,319,(1977).
- [24] C. W. Gibby, C. C. Tanner and I. Masson, Proc. R. Soc., **A122**,283,(1928).
- [25] J. A. Huff and T. M. Reed, J. Chem. Engng Data **8**,306,(1963).
- [26] G. A. Nicholson and W. G. Schneider, Can. J. Chem., **33**,589,(1955).
- [27] A. Michels, H. W. Schamp and W. de Graaff, Physica, 's Grav. **20**,1209,(1954).
- [28] G. P. Nijhoff and W. H. Keesom, Communs phys. Lab. Univ. Leiden, **179b**, (1925).
- [29] J.A. Beattie, R. J. Barriault and J. S. Brierley, J. Chem. Phys., **19**,1222,(1951).
- [30] A. Michels, T. Wassenaar and P. Louwerse, Physica, 's Grav. **20**,99,(1954).
- [31] E. Whalley, Y. Lupien and W. G. Schneider, Can. J. Chem., **33**,633,(1955).

Figure Captions

Fig. 1: A typical shape for intermolecular potential as the one given by the Lennard-Jones potential.

Fig. 2: The second virial coefficient, $B(T)$, for the Argon. The curve represents eqs.(3.12) and (3.14) - (3.16) best fitting experimental data from: \bigcirc – Holborn and Otto [5]; \square – Tanner and Masson [15]; \triangle – Walley, Lupien and Schneider [16]; ∇ – Fender and Halsey [17].

Fig. 3: The second virial coefficient, $B(T)$, for the Helium. The curves represent eqs.(3.12) and (3.14) - (3.16) best fitting experimental data from: \square – Holborn and Otto [5]; \bigcirc – White, Rubin, Camky and Johnston [18]; \triangle – Witonsky and Miller [19]; ∇ – Kalfoglou and Miller [20]. Note that eqs. (refb3) and (3.16) can not be distinguished in this graph.

Fig. 4: The second virial coefficient, $B(T)$, for the Krypton. The curve represents eqs.(3.12) and (3.14) - (3.16) best fitting experimental data from: \bigcirc – Beattie, Brierley and Barriaut [21]; \square – Walley and Schneider [22]; \triangle – Rentschler and Schramm [23].

Fig. 5: The second virial coefficient, $B(T)$, for the Hydrogen. The curve represents eqs.(3.12) and (3.14) - (3.16) best fitting experimental data from: \square – Kamerlingh Onnes and Braak [1]; \bigcirc – Holborn and Otto [5]; \triangle – Tanner and Masson [15]; ∇ – Gibby, Tanner and Masson [24].

Fig. 6: The second virial coefficient, $B(T)$, for the Nitrogen. The curve represents eqs.(3.12) and (3.14) - (3.16) best fitting experimental data from: \square – Kamerlingh Onnes and Van Urk [3]; \bigcirc – Holborn and Otto [5]; ∇ – Witonsky and Miller [19]; \triangle – Huff and Reed [25].

Fig. 7: The second virial coefficient, $B(T)$, for the Neon. The curve represents eqs.(3.12) and (3.14) - (3.16) best fitting experimental data from: \square – Holborn and Otto [5]; \bigcirc – Nicholson and Schneider [26].

Fig. 8: The second virial coefficient, $B(T)$, for the Oxygen. The curve represents eqs.(3.12) and (3.14) - (3.16) best fitting experimental data from: \square – Kuypers and H. Kamerlingh Onnes [2]; \bigcirc – Holborn and Otto [5]; ∇ – Michels, Schamp and Graaff [27]; \triangle – Nijhoff and W.H. Keesom [28].

Fig. 9: The second virial coefficient, $B(T)$, for the Xenon. The curve represents eqs.(3.12) and (3.14) - (3.16) best fitting experimental data from: \square – Beattie, Barriault and Brierley [29]; \bigcirc – Michels, Wassenaar and Louwerse [30]; \triangle – Walley, Lupien and Schneider [31].

Fig. 10: An overview of the second virial coefficients represented by eq.(3.16) as the best fit for the gases discussed in this paper. We extrapolated these functions to high temperatures in order to search for their maxima. As one can see, some of them clearly exhibits a maximum, as the case of Helium and Hydrogen; for Neon, Argon and Nitrogen they appear slightly and for the others we can not see them, at least for this range of temperatures.

| Author | Equation | $B(T)$ | T_i |
|-------------------|---|------------------------------------|-------------------------|
| Van der Waals | $PV = RT + bP - \frac{a}{V} + \frac{ab}{V^2}$ | $b - \frac{a}{RT}$ | ∞ |
| Berthelot | $PV = RT + bP - \frac{a}{TV} + \frac{ab}{TV^2}$ | $b - \frac{a}{RT^2}$ | ∞ |
| Dieterici | $PV = RT \exp(-\frac{a}{RTV}) + bP$ | $b - \frac{a}{RT}$ | ∞ |
| Redlich-Kwong | $PV = RT + bP - \frac{a}{\sqrt{T}}$ | b | $-$ |
| Beattie-Bridgeman | $PV = RT + \frac{D}{V} + \frac{E}{V^2} + \frac{F}{V^3}$ | $b - \frac{a}{RT} - \frac{c}{T^3}$ | $\sqrt{\frac{-3cR}{a}}$ |

Table 1: Equations of state and respective $B(T)$; a , b and c are different constants for each equation and gas while D , E and F are functions of T [10]. From these $B(T)$ and solving $dB/dT = 0$ one finds T_i . The only possible choice for finite T_i among these equations is the Beattie-Bridgeman equation of state. However, as a and c in this equation are positive constants for all real gases, we can see that none of the above equations lead to any real finite T_i .

| Gas | $a \times 10^5$ | $b \times 10^7$ | $c \times 10^3$ | $e \times 10^{-1}$ | $T_i(K)$ |
|----------------|-----------------|-----------------|-----------------|--------------------|----------|
| Ar | 251.00 | -2.40 | -972.00 | -345.60 | 2015 |
| He | 87.01 | -3.31 | -18.77 | - | 222 |
| H ₂ | 166.00 | -7.66 | -172.33 | - | 474 |
| N ₂ | 357.46 | -9.36 | -1044.84 | -242.53 | 1123 |
| Ne | 102.10 | -0.80 | -100.00 | -31.33 | 1259 |

Table 2: Coefficients of the eq.(3.1) for $B(T)$ from Holborn and Otto [5] and T_i calculated from eq.(3.2).

| j | T_i^* | T_{iJT}^* |
|----|-------------|-------------|
| 1 | 19.69595658 | 4.289341659 |
| 2 | 24.44023065 | 5.953282255 |
| 3 | 25.06255633 | 6.323900009 |
| 4 | 25.14189822 | 6.407536474 |
| 5 | 25.15139334 | 6.425971440 |
| 10 | 25.15257343 | 6.430797595 |
| 15 | 25.15257343 | 6.430798467 |
| 20 | 25.15257343 | 6.430798467 |

Table 3: Numerical results for the (reduced) inversion temperatures T_i^* and T_{iJT}^* corresponding to the Lennard-Jones potential.

| Gas | ϵ_0/k | $T_i(K)$ | $T_{iJT}(K)$ |
|----------------|----------------|----------|--------------|
| Ar | 119.8 | 3013 | 770 |
| He | 10.22 | 257 | 65 |
| Kr | 171 | 4301 | 1100 |
| H ₂ | 37 | 930 | 238 |
| N ₂ | 95.05 | 2391 | 611 |
| Ne | 34.9 | 878 | 224 |
| O ₂ | 118 | 2968 | 759 |
| Xe | 221 | 5558 | 1421 |

Table 4: Data for the parameter ratio ϵ_0/k of some real gases for the Lennard-Jones potential from [7] and the corresponding inversion temperatures calculated through eqs.(3.9) and (3.10).

| Gas | $T_{iJT}(K)$ | $T_i(K)$ |
|----------------|--------------|----------|
| Ar | 723 | 2827 |
| He | 40 | 156 |
| H ₂ | 204 | 797 |
| N ₂ | 625 | 2444 |
| Ne | 270 | 1055 |
| O ₂ | 750 | 2933 |

Table 5: The well known inversion temperatures T_{iJT} for the Joule-Thompson process from [13] and T_i calculated from them using eq.(3.11).

| Gas | $a \times 10^5$ | b | c | d | χ^2 | $T_i(K)$ |
|----------------|-----------------|---------|------------|----------|----------|----------|
| Ar | -3.8458 | 1.6470 | 1.4676 | -0.42510 | 39.84 | - |
| He | -0.00037874 | 0.19433 | -731.41 | 1.1205 | 7.80 | 162 |
| Kr | 12.884 | 1.7316 | 0.2639 | -0.68291 | 7.36 | - |
| H ₂ | 0.053319 | 1.1250 | 62.656 | 0.1747 | 4.77 | 762 |
| N ₂ | -1.7851 | 1.4891 | -0.075169 | 21.124 | 8.072 | - |
| Ne | 0.0009038 | 0.24146 | -3873.2 | 1.0229 | 0.99 | - |
| O ₂ | -12.758 | 1.9062 | 7.3866(-4) | -1.6421 | 3.20 | - |
| Xe | -5.8075 | 1.4302 | 20.145 | -0.11510 | 54.04 | - |

Table 6: Coefficients of eq.(3.12) fitting experimental data compiled in [4] and the corresponding T_i . See captions of figs. 2 – 9 for details concerning experimental data used in the numerical treatment for each gas.

| Gas | a | b | c | d | e | f | χ^2 | $T_i(K)$ |
|----------------|------------|---------|-------------|----------|----------|----------|----------|----------|
| Ar | -1.3342(5) | 1.4215 | -3.2404(8) | 3.6778 | 11.018 | -0.14186 | 33.10 | - |
| He | -3244.5 | 1.8348 | 5.5676 | -0.29099 | -0.79394 | -0.54227 | 3.81 | 225 |
| Kr | 6.9839(49) | 20.404 | 3.0730(6) | 1.8976 | 0.062216 | -0.88609 | 6.78 | - |
| H ₂ | -10127 | 1.0608 | 5074.5 | 1.0204 | 65.673 | 0.18220 | 4.76 | 742 |
| N ₂ | -27.083 | 1.0338 | -3.0304(10) | 4.4904 | 368.82 | 0.29037 | 6.59 | 1779 |
| Ne | -3203.8 | 0.85450 | 4.8903(-4) | -1.1751 | 426.34 | 0.43549 | 0.91 | - |
| O ₂ | 7.7283(-4) | -1.6345 | -1.2825(6) | 1.9066 | 25352 | 2.2728 | 3.20 | - |
| Xe | 8.2799(5) | 1.2173 | -1.3374(6) | 1.2710 | 2.9953 | -0.36180 | 53.67 | - |

Table 7: Coefficients of eq.(3.14) fitting experimental data compiled in [4] and the corresponding T_i . The number between parenthesis represents the decimal power of each coefficient. See captions of figs. 2 – 9 for details concerning experimental data used in the numerical treatment for each gas.

| Gas | a | b | c | d | f | g | χ^2 | $T_i(K)$ |
|----------------|------------|----------|-------------|---------|---------|---------|----------|----------|
| Ar | -1.7016 | 1.4586 | -6.6200(15) | 7.6571 | 24.387 | -1.8960 | 28.21 | - |
| He | -608.29 | 1.1845 | -2.1380(14) | 11.665 | 14.480 | 5.2356 | 2.14 | 199 |
| Kr | -1.0322(7) | 2.0942 | 1.5424(16) | 6.2812 | 7.7358 | -13.232 | 6.64 | - |
| H ₂ | -1.7658(5) | 1.2639 | 1.6979(5) | 1.2655 | 22.693 | 3.1394 | 4.58 | 574 |
| N ₂ | 42.198 | 0.050811 | -1.5131(6) | 2.0026 | -73.672 | 44.518 | 6.32 | - |
| Ne | -7354.0 | 1.2176 | 43.256 | 0.14858 | 2017.9 | 1142.3 | 0.90 | 873 |
| O ₂ | -6.6122(5) | 1.7889 | -1.5766(6) | 2.3994 | 3.5171 | -37.111 | 3.07 | - |
| Xe | -5.6145(6) | 1.7824 | 1.7444(8) | 2.6786 | 23.081 | 4.5891 | 52.82 | 1870 |

Table 8: Coefficients of eq.(3.15) fitting experimental data compiled in [4] and the corresponding T_i . The number between parenthesis represents the decimal power of each coefficient. See captions of figs. 2 – 9 for details concerning experimental data used in the numerical treatment for each gas.

| Gas | a | b | c | d | e | f | g | h | χ^2 | $T_i(K)$ |
|----------------|-------------|----------|-------------|-----------|-------------|---------|-------------|---------|----------|----------|
| Ar | -40619 | 1.0683 | -3.7726(15) | 7.4168 | 154.41 | 0.17160 | 77.936 | 48.300 | 26.47 | 3841 |
| He | -4.5828(-3) | -0.50182 | -606.47 | 1.1823 | -6.6369(15) | 12.931 | 14.540 | 5.1296 | 2.12 | 199 |
| Kr | -1.8199(6) | 1.8400 | -3.3257(8) | 2.8883 | 1.0915(13) | 4.8686 | 9.1254 | -11.701 | 6.58 | - |
| H ₂ | -123.49 | 1.1909 | 5960.4 | 1.1763 | 19.971 | 0.86958 | 23.248 | 3.5224 | 4.58 | 549 |
| N ₂ | -14734 | 0.95513 | -3.1691(7) | 2.8771 | 155.79 | 0.16280 | -9.3920(-3) | -69.007 | 6.24 | 3130 |
| Ne | -12337 | 1.3439 | 2.4123 | -0.053448 | 34.092 | 0.15637 | -128.42 | 565.23 | 0.88 | - |
| O ₂ | 4.9441(-7) | -2.8490 | -3.5770(6) | 2.1115 | 3.2702(14) | 6.5228 | -0.025554 | -85.016 | 1.90 | - |
| Xe | -1.8835(5) | 1.0629 | 2.4642(7) | 2.3383 | 239.78 | 0.10465 | 326.00 | 28.401 | 52.25 | - |

Table 9: Coefficients of eq.(3.16) fitting experimental data compiled in [4] and the corresponding T_i . The number between parenthesis represents the decimal power of each coefficient. See captions of figs. 2 – 9 for details concerning experimental data used in the numerical treatment for each gas.

| Gas | $T_i(K)$ |
|----------------|---------------------|
| Ar | $(3.8 \pm 1.8)10^3$ |
| He | $(2.0 \pm 0.5)10^2$ |
| Kr | - |
| H ₂ | $(6.6 \pm 2.7)10^2$ |
| N ₂ | $(2.5 \pm 1.4)10^3$ |
| Ne | $(8.7 \pm 3.9)10^2$ |
| O ₂ | - |
| Xe | $(1.9 \pm 0.5)10^3$ |

Table 10: Inversion temperatures T_i calculated from the numerical analysis presented in tables 6 to 9, using a χ^2 weighted average. The uncertainties were calculated taken into account T_i data from all tables 2, 4 – 9. The Krypton and Oxygen do not present inversion temperatures in this table since the experimental data available does not permit us to find them (see also fig. 10).

Fig. 1

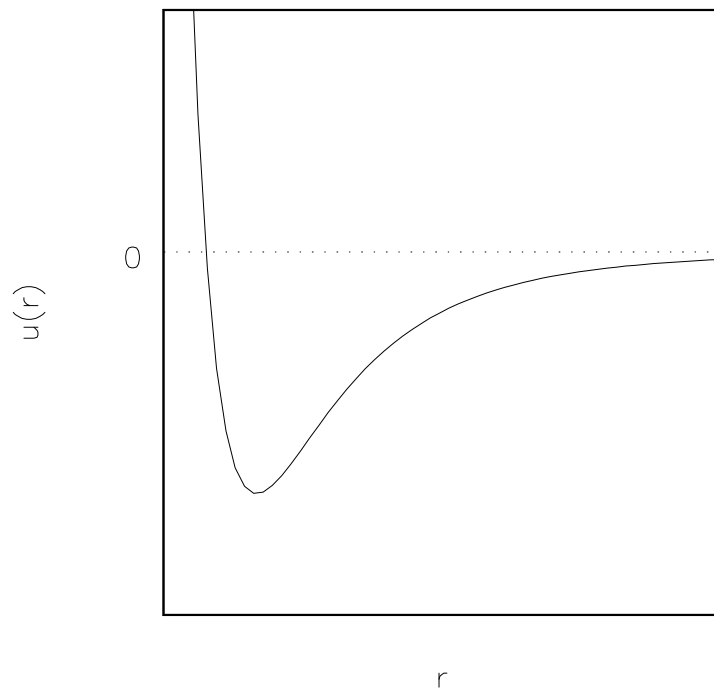


Fig. 2

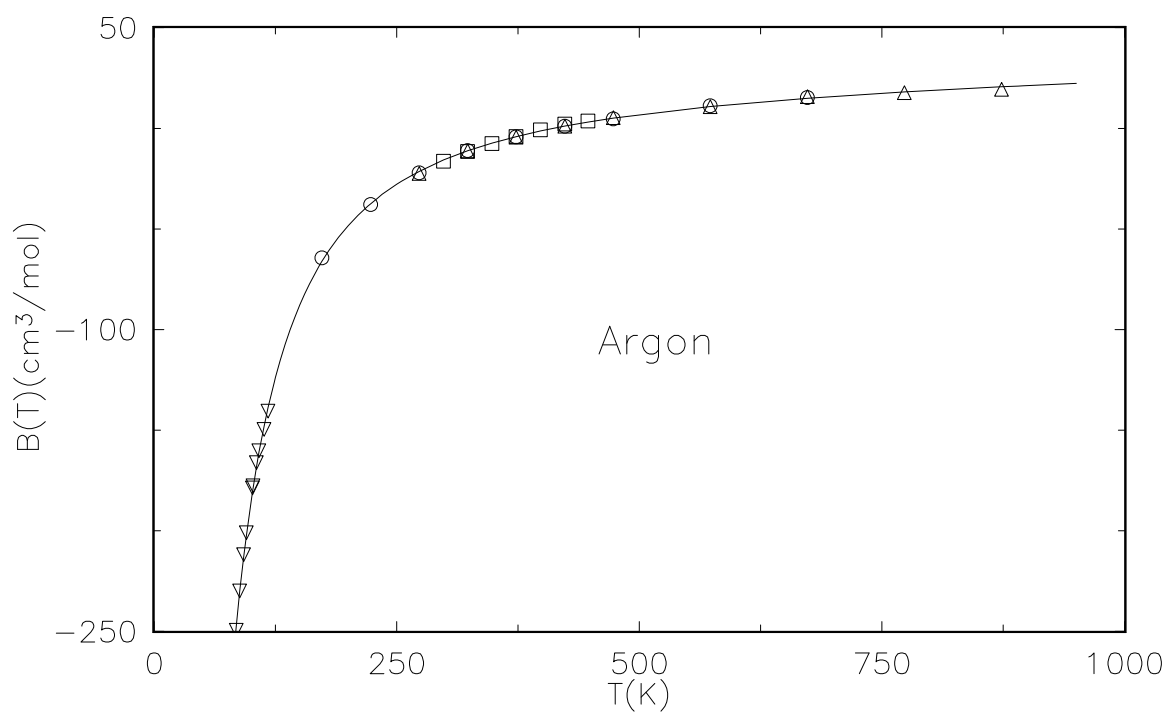


Fig. 3

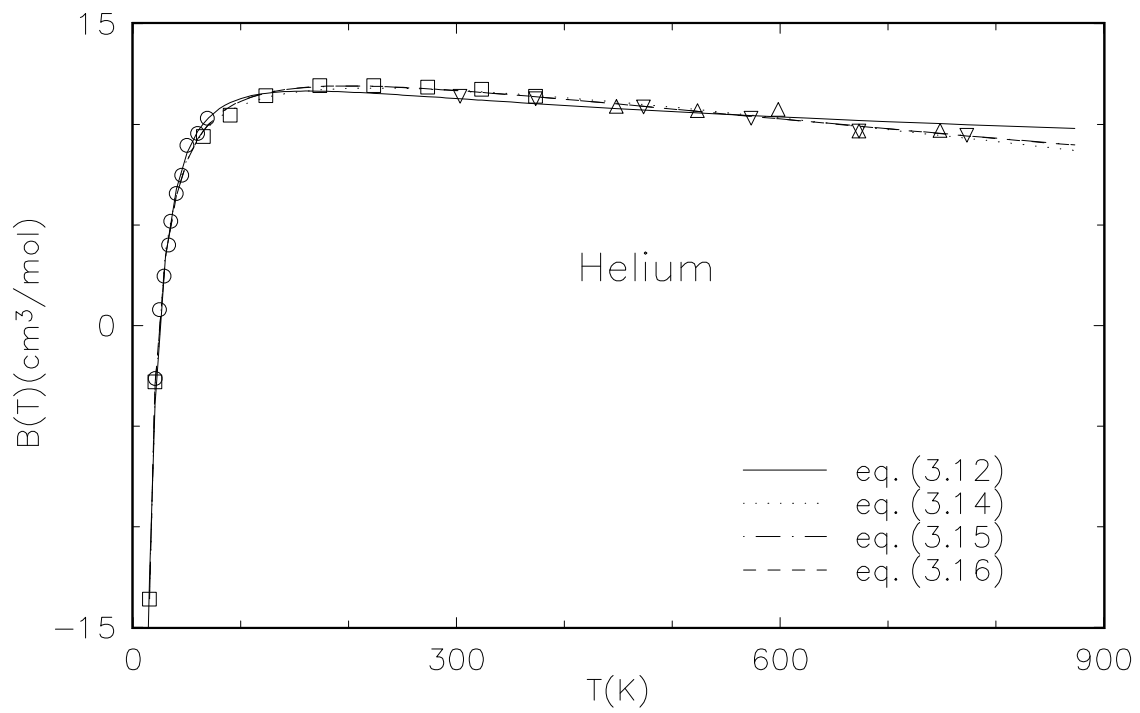


Fig. 4

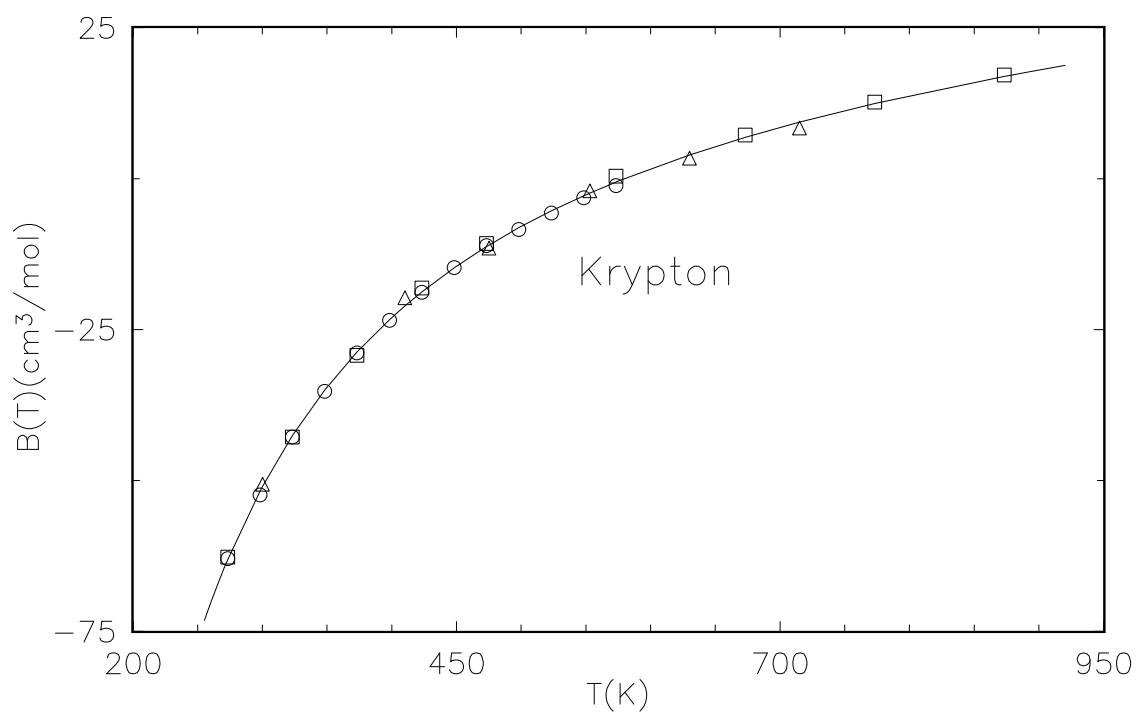


Fig. 5

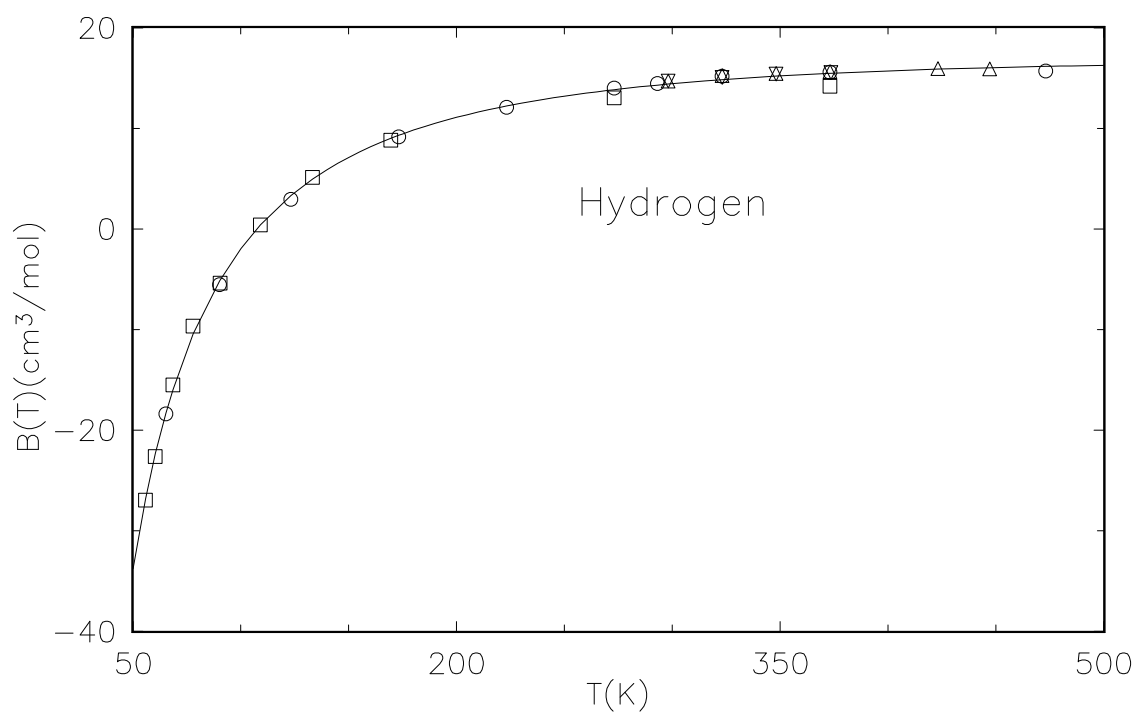


Fig. 6

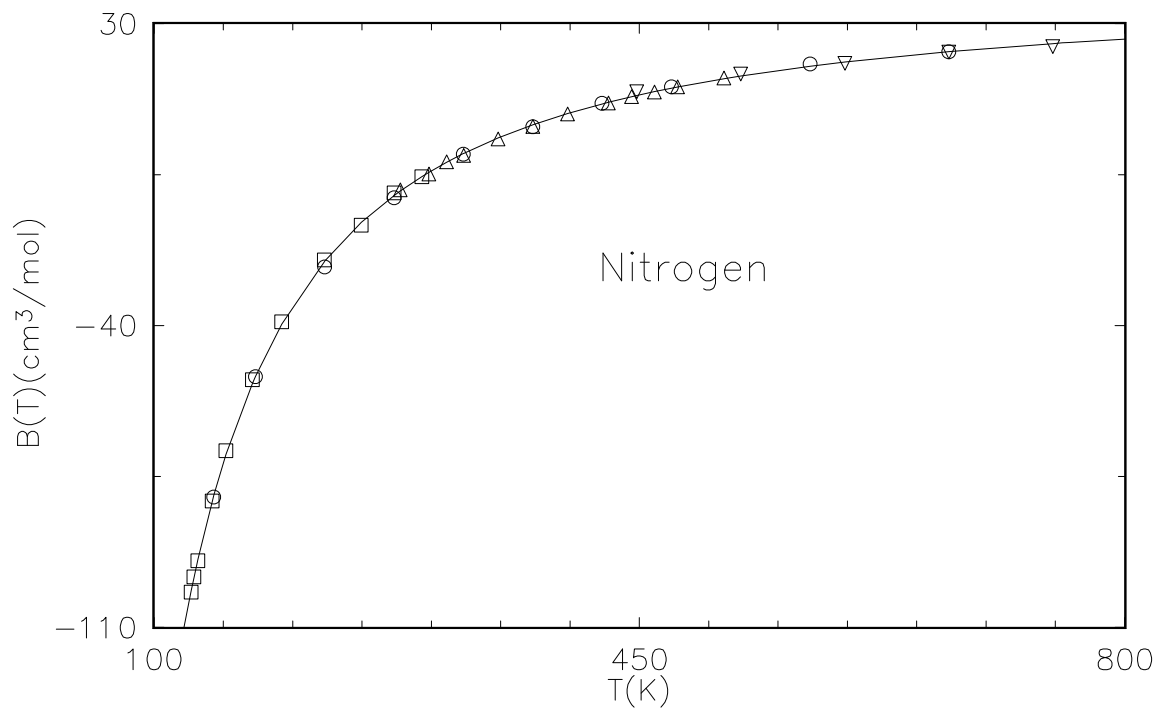


Fig. 7

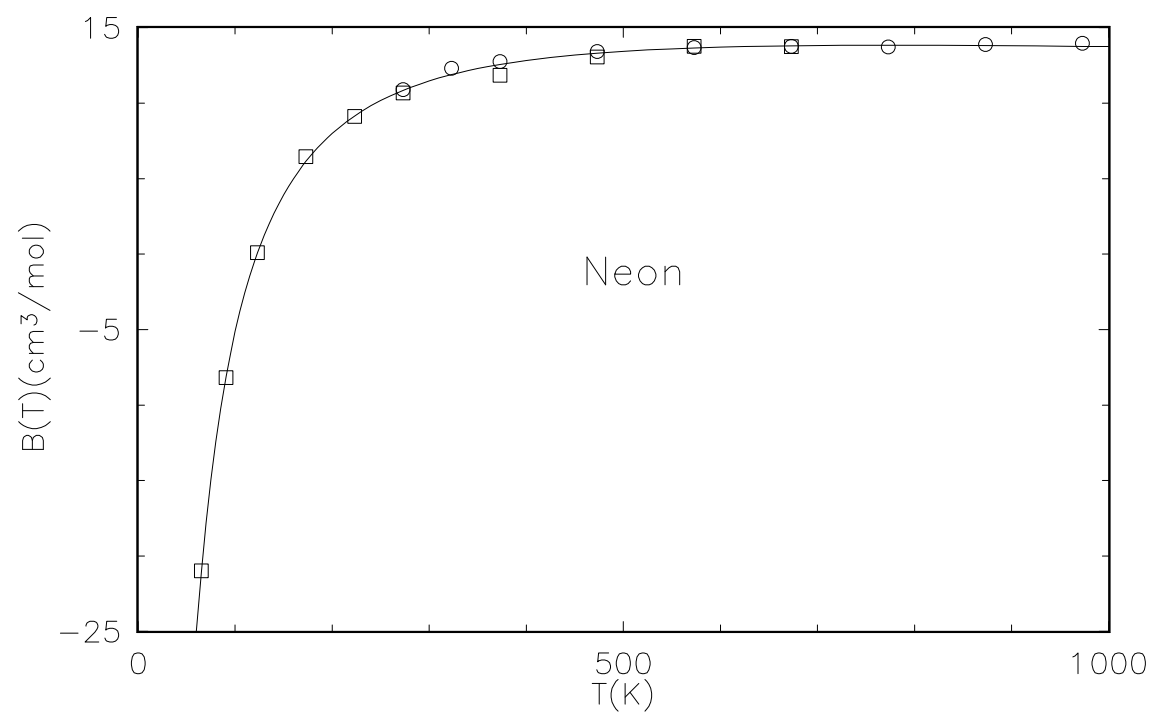


Fig. 8

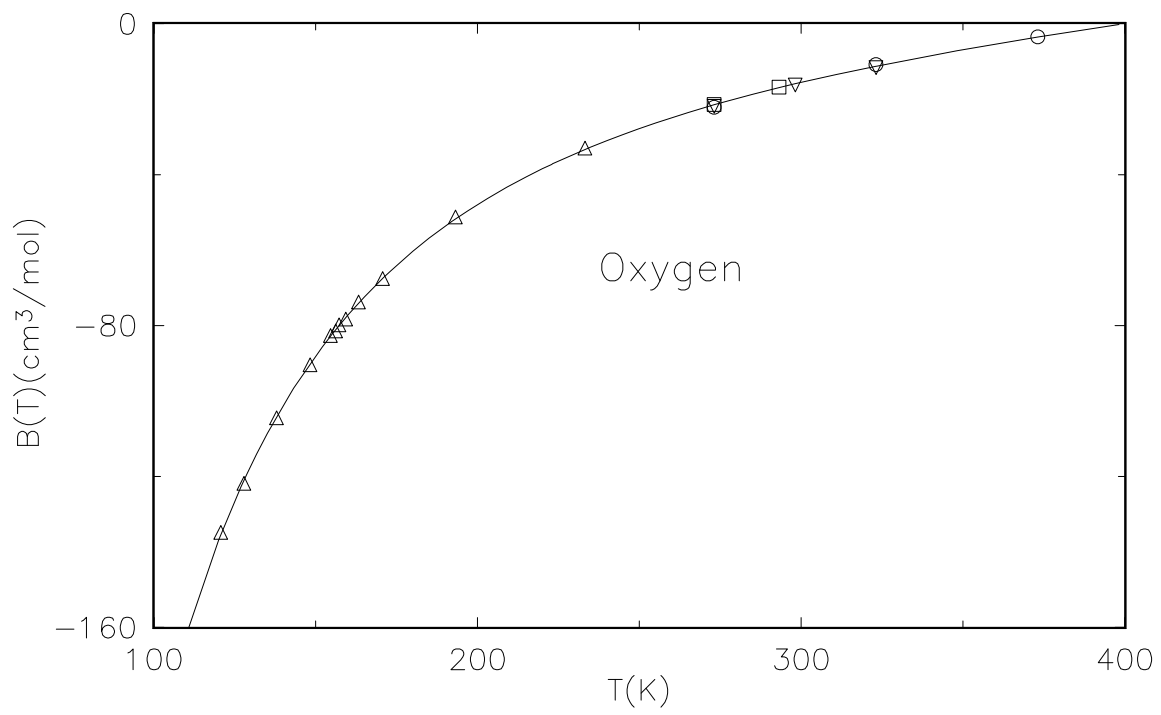


Fig. 9

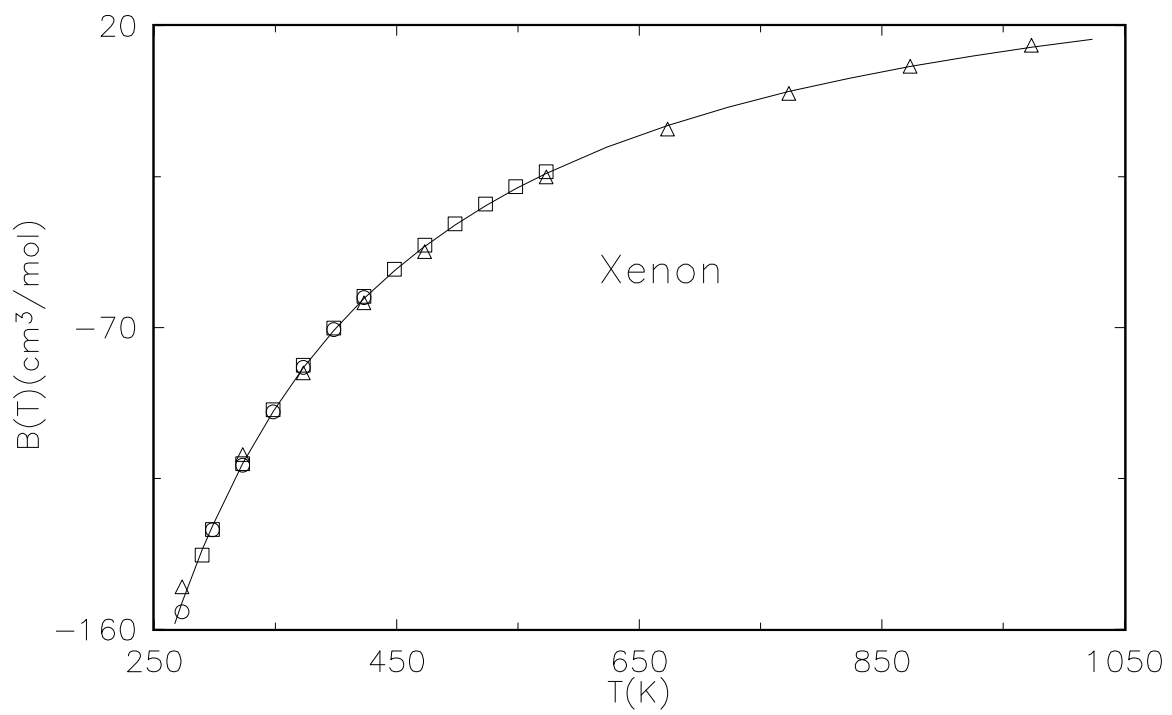


Fig. 10

